Corrosion resistance properties of superhydrophobic copper surfaces fabricated by one-step electrochemical modification process

Ying Huang[a], D.K. Sarkar[a], Danick Gallant[b], X-Grant Chen[a]

[a]University Research Center on Aluminum (CURAL), University of Québec at Chicoutimi, Chicoutimi, QC, Canada G7H 2B1

[b]Aluminum Technology Centre, National Research Council of Canada (ATC-NRC), 501, Boulevard University East, Saguenay, QC, Canada G7H 8C3
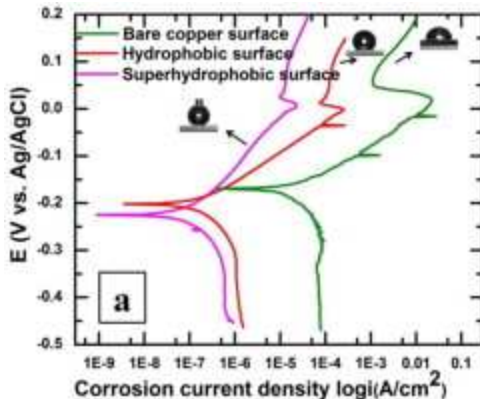
Highlights

- Superhydrophobic copper surfaces by a one-step electrochemical modification process in an ethanolic stearic acid solution.
- Analysis of the corrosion properties of as-received, hydrophobic and superhydrophobic copper surfaces.
- The corrosion resistance of the superhydrophobic surface is found to be 1220 kΩ cm^2 as compared to as-received bare copper surface 1 kΩ cm^2.

Abstract

Superhydrophobic copper surfaces have been prepared by a one-step electrochemical modification process in an ethanolic stearic acid solution. In this work, the corrosion properties of hydrophobic copper surface and superhydrophobic copper surfaces were analyzed by means of electrochemical analyses and compared with that of as-received bare copper substrate. The decrease of corrosion current density (i_{corr}) as well as the increase of polarization resistance (R_p) obtained from potentiodynamic polarization curves revealed that the superhydrophobic film on the copper surfaces improved the corrosion resistance performance of the copper substrate.

Graphical Abstract

1. Introduction

Copper has been one of the important materials, which is widely used in many applications such as a conductor in electrical power lines and pipelines for domestic and industrial water utilities including seawater, heat conductors and heat exchangers [1]. Therefore, the corrosion prevention of copper has attracted attention of a number of investigators [2], [3], [4], [5] and [6].

It is well known that the contact of metals with water triggers the corrosion reactions. Thus, the corrosion resistance of copper can be significantly improved by reducing the contact area of water with copper surfaces. This goal can be achieved by transforming as-received bare copper surfaces to superhydrophobic copper surfaces. Fabrication of superhydrophobic surfaces, with water contact angle larger than 150°, where water drops roll of easily even with the slightest surface inclination, is inspired by the nature which presents numerous surfaces such as lotus leaves that are inherently water-repellent [7] and [8]. An optimized surface topography and low surface energy are generally the two important requirements for the fabrication of superhydrophobic surfaces [9] and [10]. Recently, superhydrophobic coatings have been applied to various engineering material surfaces such as steel, copper, zinc, and aluminum, to improve their corrosion resistance performances [11], [12], [13], [14], [15] and [16], Our research team has prepared superhydrophobic surfaces using many techniques such as chemical bath deposition (CBD) [17], substrate chemical etching [18], galvanic exchange reaction [19], electrochemical deposition [20], etc. The employed techniques mostly are two-step procedures which involves creation of an optimum micro-nanoroughness as a first step and modifying the created surfaces further to lower their surface energies as a second

subsequent step to reduce the affinity of water thereby weakening the water–surface interactions [17], [18], [21], [22], [23] and [24]. In our recent studies, we have developed one-step process to obtain various superhydrophobic surfaces by simplifying the complexity of two-steps process [19], [20], [25], [26] and [27]. Among the various one-step processes to fabricate superhydrophobic surfaces, we have accomplished the fabrication of superhydrophobic copper surfaces by simply immersing the copper electrodes in the stearic acid solution with the application of DC voltage [20].

In the present studies, considering the importance of corrosion resistance of the copper surfaces, the corrosion properties of the superhydrophobic copper surfaces fabricated by the one-step process has been investigated and compared with that of the as-received bare copper substrate utilizing the potentiodynamic polarization technique. Further investigation on the morphological, chemical compositional and non-wetting performance of the surfaces exposed to corrosive medium demonstrated the anti-corrosive properties of the superhydrophobic copper surfaces.

2. Experimental

One-inch-square copper substrates were ultrasonically cleaned in a soap solution for 30 min for degreasing, followed by oxide removal by immersing in 10 vol.% HNO_3 and rinsing in water and ethanol. The cleaned substrates were electrochemically modified in an ethanolic stearic acid solution (0.01 M) with a DC voltage of 30 V for a range of time. Using two electrodes configuration, the anodic and cathodic copper plates were separated by a distance of 1.5 cm. The morphological and elemental analyses of the anodic copper surfaces were performed using a scanning electron microscope (SEM, JEOL JSM-6480 LV). The chemical composition of surfaces is analyzed by X-ray diffraction (XRD, D8 discover) in a standard θ–2θ mode and infrared reflection absorption spectroscopy (IRRAS, Nicolet 6700FT-IR). The wetting characteristics of the sample surfaces were carried out by measuring both static and dynamic contact angles using a First Ten Angstrom contact angle goniometer at five positions on each substrate using 10 µL deionized water drop. The dynamic contact angle was measured by holding the water drop with a stationary needle in contact with the sample surface and moving the goniometer stage in one direction. The static contact angle has been abbreviated as WCA and dynamic contact angle or contact angle hysteresis has been abbreviated as CAH throughout the text [18] and [28]. The adhesion of copper stearate on copper

substrate were carried out according to the ASTM D3359 standard test method using Cross Hatch Cutter, model Elcometer 107.

The corrosion resistance of the samples was investigated via potentiodynamic polarization curves acquired by electrochemical experiments in a 3.5% NaCl solution (natural pH 5.9). The time of open circuit potential (OCP) and polarization studies were 40 min and approximately six minutes respectively, for all samples. Electrochemical experiments were performed using a PGZ100 potentiostat and a 300 cm^3 – EG&G PAR flat cell (London Scientific, London, ON, Canada), equipped with a standard three-electrode system with an Ag/AgCl reference electrode, a platinum (Pt) mesh as the counter electrode (CE), and the sample as the working electrode (WE) [25] and [29].

3. Results and discussion

Various hydrophobic (water contact angle (WCA) > 90°) and superhydrophobic (WCA > 150°) copper surfaces were fabricated by electrochemical modification via immersion of the copper substrates in ethanolic stearic acid solution at 30 V DC for the durations of 15, 30, 60, 90, 105 and 120 min. The anodic electrode of copper surfaces transformed to copper stearate following electrochemical modification as observed from the low angle XRD pattern shown in Fig. 1(a). The four distinct peaks appearing in the spectra are assigned to copper stearate ($CH_3(CH_2)_{16}COO)_2Cu$ [30] resulting from a reaction between stearic acid ($CH_3(CH_2)_{16}COOH$) and copper upon application of DC voltage. The appearance of the copper stearate peaks in the XRD patterns confirms the presence of low surface energy methylated (CH_3 and CH_2) components on the copper surfaces [20]. The XRD patterns show that the prominent peaks attributed to copper stearate as shown in Fig. 1(a) increases in intensity with the electrochemical modification time.
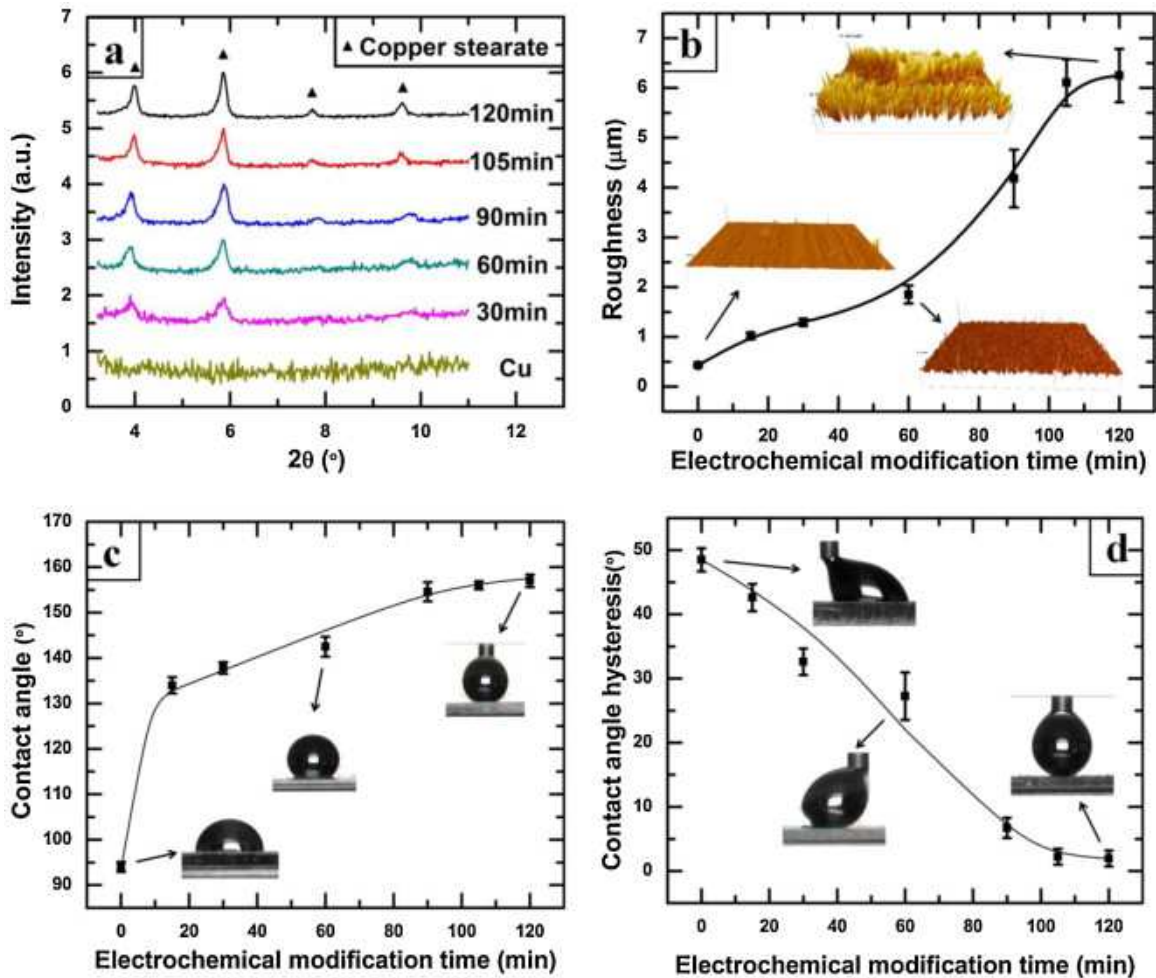
Fig. 1. (a) XRD patterns of as-received bare copper surface and copper surfaces after electrochemical modification with stearic acid solution at 30 V DC between 30 and 120 min. (b) Variation of surface roughness, (c) water contact angle and (d) contact angle hysteresis. The inset images of (b) shows the morphology of the surfaces. The inset images of (c) and (d) show the water drop shape on the respective surfaces.

Fig. 1(b) depicts the variation of surface roughness of anodic copper surfaces after electrochemical modification for the durations of 15–120 min. The surface roughness 0.43 μm on as-received bare copper surface was found to increase to 1.02 μm, 1.29 μm and 1.85 μm following electrochemical modification for 15, 30 and 60 min, respectively. The increase in the roughness values is due to the formation of copper stearate on the anodic copper surface as revealed by the XRD analysis. However, the surface roughness of the anodic copper surface due to electrochemical modification for 90 min increased drastically to a very high value of 4.18 μm. With further increase of

electrochemical modification time to 105 and 120 min, surface roughness increased to 6.11 and 6.25 µm, respectively.

Static and dynamic contact angle measurements were carried out on these surfaces to evaluate the wetting characteristics. Fig. 1(c) and (d) shows the variation of water contact angle (WCA) and contact angle hysteresis (CAH) of the copper surfaces as a function of electrochemical modification times. It is evident from these measurements that as-received bare copper surface has a water contact angle of 94°. The water contact angle increased to 134° with contact angle hysteresis of 42° following electrochemical modification for 15 min. The copper surface becomes superhydrophobic providing WCA of 155° and CAH of 6° after an electrochemical modification for 90 min. Further increase of modification time to 105 and 120 min leads to very slight increase of WCA of 157°, with a decrease of CAH to 2° in both cases.

It is important to mention that the mechanical properties of the superhydrophobic coatings are very important for their uses against surface erosion, friction as well as corrosion protection [31], [32], [33] and [34]. The typical hardness of the superhydrophobic coatings varies in the range of 2H to 9H and their adhesion strength is approximately 5B [34]. Keeping these important applications in mind, have carried out the adhesion test using the same experimental set up as described by Lakshmi et al. however, our results are very random and varies between 3B and 5B.

Fig. 2 shows the potentiodynamic polarization curves of the as-received bare copper surface, electrochemically modified hydrophobic and superhydrophobic copper surfaces enriched with copper stearate.
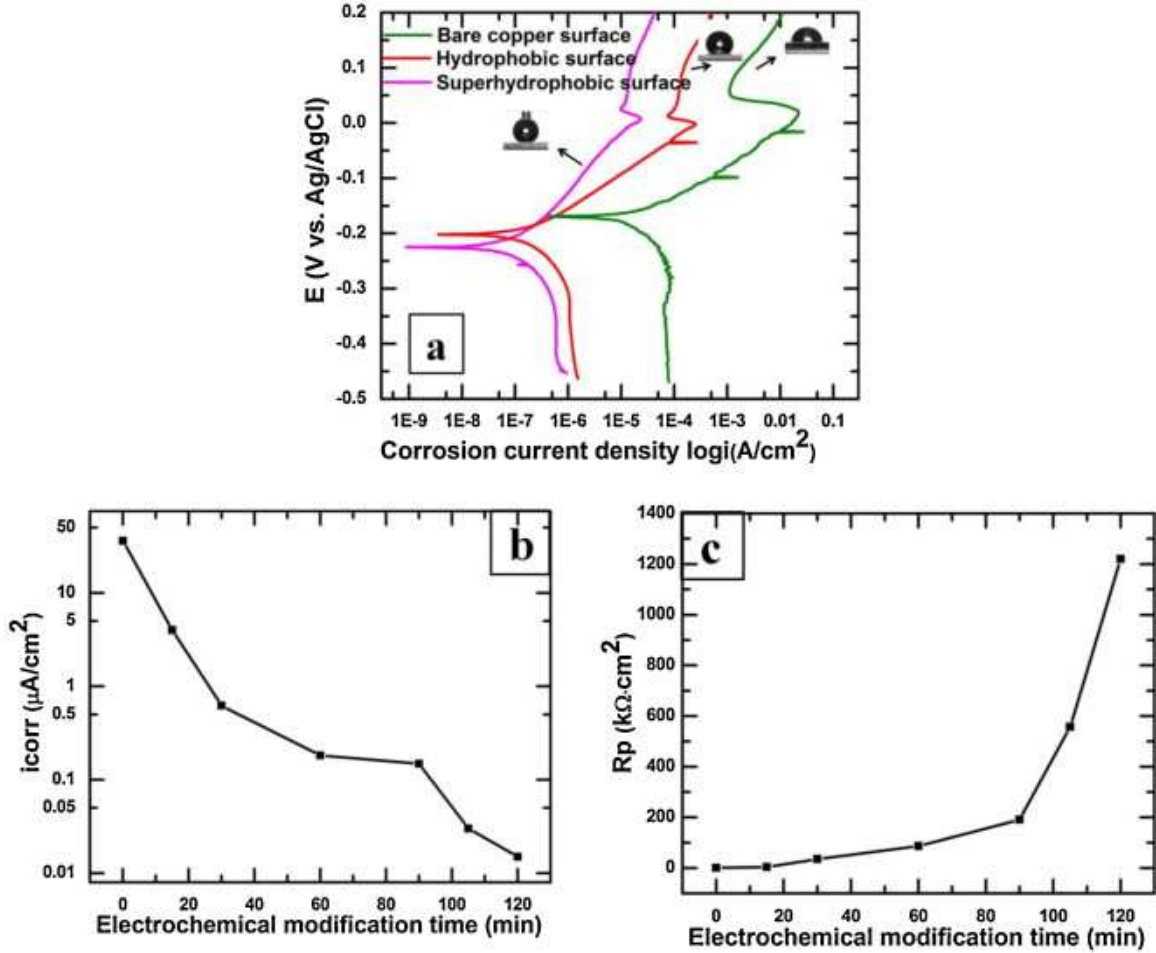
Fig. 2. (a) Potentiodynamic curves of as-received bare copper surface, hydrophobic copper surface and superhydrophobic copper surface. The insets show the water drops on each surface. (b) Variation of corrosion current density and (c) polarization resistance as a function of the electrochemical modification time at 30 V DC voltage in ethanolic stearic acid solution.

Fig. 2 shows the potentiodynamic polarization curves, i.e., corrosion current density vs. corrosion potential, of the as-received bare, hydrophobic and superhydrophobic copper surfaces. Generally, polarization resistance (R_p), is calculated from the corrosion current density (i_{corr}), using Stern–Geary equation [35], given by Eq. (1):

Equation (1)

$$R_p = \frac{\beta_a \beta_c}{2.3 i_{corr}(\beta_a + \beta_c)}$$

where β_a and β_c are anodic and cathodic Tafel slopes, respectively.

However, the integrated software with the potentiostat is capable to calculate β_a, β_c as well as i_{corr} from the polarization curves as presented in Fig. 2(a). The software is also capable to determine the R_p using Eq. (1). Fig. 2(a) shows the corrosion current density (i_{corr}) of the as-received bare copper substrate having contact angle of ~94° is found to be 36.10 µA/cm^2. The copper substrate after passivation with stearate acid has a contact angle of ~118° and corrosion current density of 11.4 µA/cm^2. The corrosion current density of these surfaces, when rendered hydrophobic upon electrochemical modification exhibiting a water contact angle of 138°, reduced to 0.62 µA/cm^2. The corrosion current density further reduced remarkably to 0.01 µA/cm^2 on the superhydrophobic copper surface which exhibited a very high water contact angle of 157°. These investigations show that the electrochemically modified copper surfaces in ethanolic stearic acid solutions exhibit anticorrosion properties as compared to as-received bare copper surfaces.

Above all, the stearic acid modified copper surfaces with superhydrophobic properties demonstrate higher protection against corrosion than its hydrophobic counterpart. Fig. 2(b) and (c) shows the variation of corrosion current density and the polarization resistance of the copper surfaces with the electrochemical modification time in the ethanolic stearic acid solution. It is clear from these graphs that the corrosion current density has reduced drastically with the increase of modification time and consequently, resulting in an increase in the polarization resistance. The wetting and corrosion properties, including contact angle, corrosion current density as well as polarization resistance of as-received bare copper surface as well as hydrophobic and superhydrophobic surfaces also have been summarized in Table 1.

Table 1. Water contact angle values and their respective corrosion current density and polarization resistance values as derived from Fig.2(a) for the surfaces modified electrochemical for varying modification times.

Surface electrochemical modification time at 30 V (min)	Water contact angle (°)		Corrosion current density, i_{corr} ($\mu A/cm^2$)	Polarization resistance, R_p ($k\Omega\ cm^2$)
	Before corrosion	After corrosion		
Bare copper	94 ± 1	84 ± 1	36.10	1
Passivated copper with SA	118 ± 1	101 ± 1	11.3	1.25
15	134 ± 2	118 ± 2	4.00	3
30	138 ± 1	125 ± 2	0.62	35
60	142 ± 2	135 ± 2	0.18	86
90	155 ± 2	154 ± 2	0.15	191
105	156 ± 1	155 ± 1	0.03	557
120	157 ± 1	156 ± 1	0.01	1220

It is clear from Fig. 2(c) as well as from Table 1 that the copper surface provides very low polarization resistance of 1 $k\Omega\ cm^2$. However, the hydrophobic copper surface composed of copper stearate following a modification time of 30 min exhibiting a water contact angle value of ~138°, provides higher polarization resistance of 35 $k\Omega\ cm^2$. In contrast, the corrosion resistance is just 1.25 $k\Omega\ cm^2$ for copper surface passivated with stearic acid without any external potential. Increasing the modification times to 90 min results in an increased polarization resistance of 191 $k\Omega\ cm^2$ which may be due to the superhydrophobic properties of these surface having a water contact angle of 155°. With further increase of modification time to 105 min and 120 min, the polarization resistances drastically increase to 557 $k\Omega\ cm^2$ and 1220 $k\Omega\ cm^2$, respectively, although water contact angles on these two surfaces remains similar (156° and 157°, respectively) and comparable to that obtained on the surface modified for 90 min. This drastic increase of polarization resistance may be attributed to the combination of the superhydrophobic properties along with higher thickness of the copper stearate films, as evidenced from the increase of XRD peak height of copper stearate with the modification time as shown in Fig. 1(a).

The polarization resistance is an important parameter to evaluate the anti-corrosion performance of materials as higher the polarization resistance indicates higher anti-corrosion properties. Liu et al. studied the corrosion properties of superhydrophobic copper surfaces prepared by creating rough copper surfaces in the first step and then passivating with n-tetradecanoic (myristic) acid for 10 days [16]. They reported on their superhydrophobic copper surface that the corrosion current density and the polarization

resistance were 0.4 $\mu A/cm^2$ and 40 $k\Omega\ cm^2$, respectively. On the other hand, the corrosion current density and the polarization resistance were 3 $\mu A/cm^2$ and of 1.7 $k\Omega\ cm^2$, respectively, on their as-received bare copper substrate. Similarly, Yuan et al. also used a two step process to create superhydrophobic surfaces by etching copper to create the rough surface and further lowering the surface energy using hexafluorobutyl acrylate molecules [14]. In their studies, the corrosion current density was found to be 1.61 $\mu A/cm^2$ and the polarization resistance was found be around 200 $k\Omega\ cm^2$ on their superhydrophobic surfaces. However, they found very high corrosion current density of 34 $\mu A/cm^2$ and very low the polarization resistance of 5.9 $k\Omega\ cm^2$ on the as-received bare copper substrates. Nonetheless, in our experiments, we have found that a much higher polarization resistance as well as a much lower corrosion current density on our superhydrophobic copper surfaces prepared by a one-step electrochemical modification process as compared to the values reported by reported by Liu et al. [16] and Yuan et al. [14] on their superhydrophobic copper surfaces prepared using two-step procedure. Furthermore, in a study by Liu et al. [11], superhydrophobic zinc films were prepared by a simple immersion technique into a fluorochlorosilane solution for 5 days at room temperature followed by a short annealing at 130 °C in air for an hour. Their superhydrophobic coatings were used to protect zinc surfaces where the authors reported a corrosion current density of 0.16 $\mu A/cm^2$ and the calculated polarization resistance was found to be 140 $k\Omega\ cm^2$. On the other hand they found that the corrosion current density and polarization resistance of the pure zinc surfaces were 10.9 $\mu A/cm^2$ and 20 $k\Omega\ cm^2$, respectively. It is clear from these studies as well as our findings that the superhydrophobic surfaces have the potential to protect metals against corrosion.

Further, SEM has been utilized to monitor the morphological changes on the as-received bare, hydrophobic and superhydrophobic copper surfaces after the corrosion tests. Fig. 3 shows the SEM images of the as-received bare, hydrophobic and superhydrophobic copper surfaces before and after corrosion test. Comparison between the SEM images of as-received bare copper surface before and after corrosion test (Fig. 3(a) and (b)) clearly indicates the formation of corrosion pits as marked by arrows in Fig. 3(b). It was found that following corrosion tests, the WCA on the as-received bare copper surfaces decreased to 84° from 94° obtained before corrosion tests. The insets of Fig. 3(a) and (b) show the image of a water droplet on the respective surfaces. The decrease of water contact angle after corrosion test might be due to the presence of corrosion products

such as CuCl$_2$ as the corrosive medium used in the tests is a NaCl solution [36]. Fig. 3(c) and (d) represents the hydrophobic copper surface before and after corrosion test, respectively. Surface morphology prior to corrosion test on these surfaces is very similar to that of the as-received bare copper surface. Similarly, formation of corrosion pits is also evident (Fig. 3(d) following corrosion test on these surfaces as observed on the as-received bare copper surfaces. However, the diameter of the corrosion pits on the hydrophobic copper surfaces is found to be much smaller than those formed on the as-received bare copper surfaces. It has been found that the water contact angle of hydrophobic copper surface reduced to 135° from 142° after the corrosion test similar to that observed on the as-received bare copper surfaces. Fig. 3(e) and (f) shows the surface morphology of the superhydrophobic copper surfaces before and after corrosion tests. Fig. 3(e) reveals the formation of micro-size flower-like particles on the superhydrophobic copper surfaces confirmed to be copper stearate from the XRD investigations (Fig. 1(a)) Fig. 3(f) shows the surface morphology of these superhydrophobic copper surfaces after the corrosion test. Unlike the as-received bare and hydrophobic copper surfaces, the superhydrophobic copper surfaces do not reveal any pits formation following corrosion test. The water contact angle of superhydrophobic surface has been found to remain similar maintaining the superhydrophobic properties as the water drops were found to roll-off easily on these surfaces as observed before corrosion. However, the SEM image of these surfaces following corrosion test (Fig. 3(f)) reveals a minor change in the morphological features as it can be noticed that the number of the flower-like features decreased slightly. Therefore, in order to understand if the exposure of the superhydrophobic copper surfaces to the corrosive medium has had any influence on the chemical nature of the surface, IRRAS spectra as well as XRD patterns were acquired on these surfaces prior to and after corrosion tests.
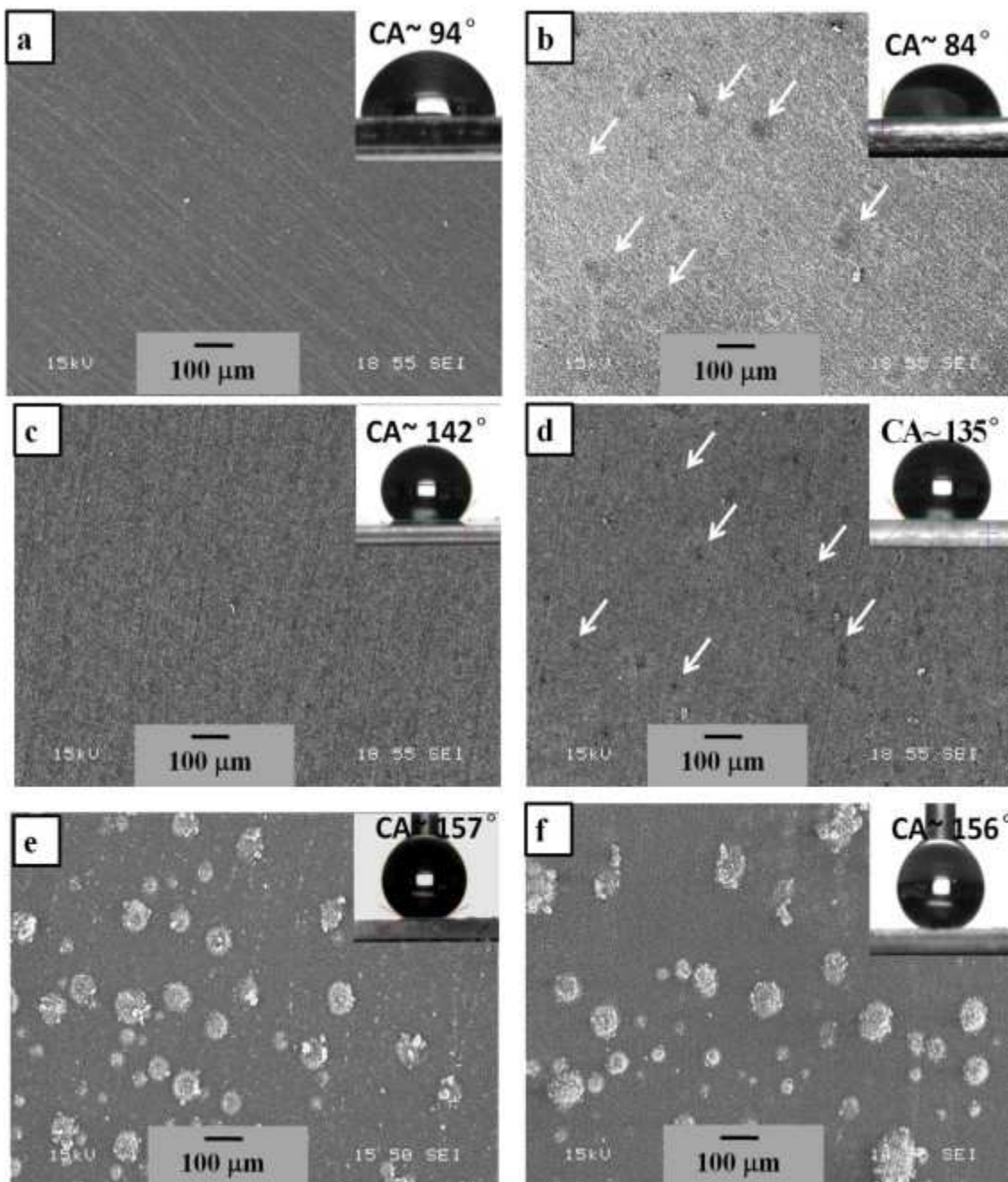
Fig. 3. SEM images of (a) pure copper surface before corrosion test and (b) pure copper after corrosion; (c) hydrophobic copper surface before corrosion test and (d) hydrophobic copper surface after corrosion test; (e) superhydrophobic copper surface before corrosion test and (f) superhydrophobic copper surface after corrosion test. Arrows in (b) and (d) show the corrosion pits on the surfaces.

The IRRAS spectra of the superhydrophobic copper surfaces prior to and after corrosion tests confirmed the presence of copper stearate on the surface as well as its stability

after corrosion test showing no changes in the surface chemistry. As presented in Fig. 4(a), the two peaks at wavenumbers 2851 and 2922 cm^{-1} belongs to the symmetric and asymmetric C—H stretching modes of —CH$_2$ groups of copper stearate, respectively, and the peak at 2955 cm^{-1} is ascribed to the asymmetric in-plane C–H stretching mode of the –CH$_3$ group [17]. The peaks at 1470 and 1583 cm^{-1} are also observed which are ascribed to the symmetric and asymmetric –COO, respectively, arising from copper stearate molecules [30]. The IRRAS spectra of superhydrophobic copper surface before and after corrosion test show similar characteristics, which is in close agreement with the copper stearate peaks appearing in the XRD patterns (as shown in Fig. 4(b)). The stable micro-nanostructured low surface energy copper stearate surface did not greatly alter the water contact angle of the surface following exposure to NaCl solutions in the corrosion tests maintaining the superhydrophobic properties.
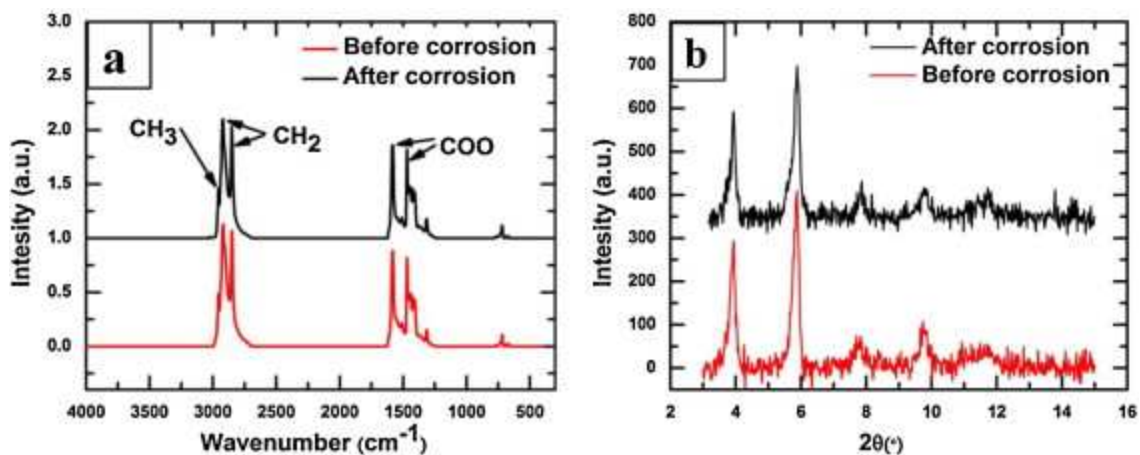

Fig. 4. (a) The IRRAS spectra showing —CH$_2$, —CH$_3$ and —COO peaks of copper stearate before and after corrosion tests. (b) The XRD patterns of superhydrophobic copper surface before and after corrosion test.

4. Conclusions

The superhydrophobic copper surfaces were fabricated by immersing the anodic copper surface in the stearic acid solution at 30 V DC. The anodic copper surface transformed

to superhydrophobic due to the formation of copper stearate. The corrosion resistance of the superhydrophobic surface is found to be 1220 kΩ cm^2 as compared to as-received bare copper surface 1 kΩ cm^2. The surface morphological analysis, before and after corrosion test, has been conducted to evaluate the corrosion performance. The as-received bare copper surfaces show the formation of pits due to corrosion. On the other hand, no visible corrosion pits are observed on the superhydrophobic surfaces. Furthermore, the morphological, chemical compositional and wetting behavior analysis show that the superhydrophobic surfaces are stable against exposure to corrosive medium as the micro–nano morphological features as well as the molecular structure is not greatly altered following corrosion tests.

References

[1] L. Nunez, E. Regura, F. Corvo, E. Gonzalez, C. Vazquez
Corrosion Science, 47 (2005), p. 461
[2] J.C. Hamilton, J.C. Farmer, R.J. Anderson
Journal of The Electrochemical Society, 133 (1986), p. 739
[3] E. Rocca, G. Bertrand, C. Rapin, J.C. Labrune
Journal of Electroanalytical Chemistry, 503 (2001), p. 133
[4] K. Rhattas
Materials Sciences and Applications, 2 (2011), p. 220
[5] A. Romeiro, C. Gouveia-Caridade, C.M.A. Brett
Corrosion Science, 53 (2011), p. 3970
[6] A. Robin, G.A.S. Martinez, P.A. Suzuki
Materials & Design, 34 (2012), p. 319

[7] A. Lafuma, D. Quere

Nature Materials, 2 (2003), p. 457

[8] X. Gao, L. Jiang

Nature, 432 (2004), p. 36

[9] X. Feng, L. Feng, M. Jin, J. Zhai, L. Jiang, D. Zhu

Journal of American Chemistry Society, 126 (2004), p. 62

[10] N. Verplanck, Y. Coffinier, V. Thomy, R. Boukherroub

Nanoscale Research Letters, 2 (2007), p. 577

[11] H.Q. Liu, S. Szunerits, W.G. Xu, R. Boukherroub

ACS Applied Materials & Interfaces, 1 (2009), p. 1150

[12] W.J. Xu, J.L. Song, J. Sun, Y. Lu, Z.Y. Yu

ACS Applied Materials & Interfaces, 3 (2011), p. 4404

[13] Q. Zhang, Y.R. Zhu, Z.Y. Huang

Chemical Journal of Chinese Universities-China, 30 (2009), p. 2210

[14] S.J. Yuan, S.O. Pehkonen, B. Liang, Y.P. Ting, K.G. Neoh, E.T. Kang

Corrosion Science, 53 (2011), p. 2738

[15] T. Ning, W.G. Xu, S.X. Lu

Applied Surface Science, 258 (2011), p. 1359

[16] J. Li, X. Liu, Y. Ye, H. Zhou, J. Chen

Applied Surface Science, 258 (2011), p. 1772

[17] N. Saleema, M. Farzaneh

Applied Surface Science, 254 (2008), p. 2690

[18] D.K. Sarkar, M. Farzaneh, R.W. Paynter

Materials Letters, 62 (2008), p. 1226

Loading

[19] D.K. Sarkar, R.W. Paynter

Journal of Adhesion Science and Technology, 24 (2010), p. 1181

[20] Y. Huang, D.K. Sarkar, X.G. Chen

Materials Letters, 64 (2010), p. 2722

[21] A. Safaee, D.K. Sarkar, M. Farzaneh

Applied Surface Science, 254 (2008), p. 2493

[22] D.K. Sarkar, M. Farzaneh

Journal of Adhesion Science and Technology, 23 (2009), p. 1215

[23] D.K. Sarkar, M. Farzaneh, R.W. Paynter

Applied Surface Science, 256 (2010), p. 3698

[24] J.D. Brassard, D.K. Sarkar, J. Perron

ACS Applied Materials & Interfaces, 3 (2011), p. 3583

[25] N. Saleema, D.K. Sarkar, D. Gallant, R.W. Paynter, X.G. Chen

ACS Applied Materials & Interfaces, 3 (2011), p. 4775

[26] D.K. Sarkar, N. Saleema

Surface and Coatings Technology, 204 (2010), p. 2483

[27] N. Saleema, D.K. Sarkar, R.W. Paynter, X.G. Chen

ACS Applied Materials & Interfaces, 2 (2010), p. 2500

[28] J.D. Brassard, D.K. Sarkar, J. Perron

Applied Science, 2 (2012), p. 453

[29] Y. Han, D. Gallant, X.G. Chen

Corrosion, 67 (2011), p. 115005

[30] Copper stearate JCPDS # [00-055-1622].

[31] Q. Ke, W. Fu, H. Jin, L. Zhang, T. Tang, J. Zhang

Surface and Coatings Technology, 205 (2011), p. 4910

[32] R.V. Lakshmi, T. Bharathidasan, B.J. Basu

Applied Surface Science, 257 (2011), p. 10421

[33] J. Ou, M. Liu, W. Li, F. Wang, M. Xue, C. Li

Applied Surface Science, 258 (2012), p. 4724

[34] R.V. Lakshmi, T. Bharathidasan, P. Bera, B.J. Basu

Surface and Coatings Technology, 206 (2012), p. 3888

[35] M. Stern, A.L. Geary

Journal of The Electrochemical Society, 104 (1957), p. 56

[36] G. Kear, B.D. Barkar, F.C. Walsh

Corrosion Science, 46 (2004), p. 109